Thermoreversible Cross-Linking of Maleated Ethylene/Propylene Copolymers Using Hydrogen-Bonding and Ionic Interactions

ARTICLE *in* MACROMOLECULES · MAY 2006

Impact Factor: 5.8 · DOI: 10.1021/ma052691v

4 AUTHORS, INCLUDING:

Chunxia Sun
Royal DSM
1 PUBLICATION **24** CITATIONS
SEE PROFILE

J. G. P. Goossens
Technische Universiteit Eindhoven
98 PUBLICATIONS **1,328** CITATIONS
SEE PROFILE

M. van Duin
LANXESS, Geleen, Netherlands
142 PUBLICATIONS **2,495** CITATIONS
SEE PROFILE

Thermoreversible Cross-Linking of Maleated Ethylene/Propylene Copolymers Using Hydrogen-Bonding and Ionic Interactions

C. X. Sun,[†,‡] M. A. J. van der Mee,[‡,§] J. G. P. Goossens,*[,‡,§] and M. van Duin[⊥]

Department of Macromolecular Science, The Key Laboratory of Molecular Engineering of Polymers, Fudan University, Shanghai 200433, People's Republic of China; Laboratory of Polymer Technology, Department of Chemical Engineering and Chemistry, Eindhoven University of Technology, PO Box 513, 5600 MB Eindhoven, The Netherlands; Dutch Polymer Institute, PO Box 902, 5600 AX Eindhoven, The Netherlands; and DSM Research, PO Box 18, 6160 MD Geleen, The Netherlands

Received December 16, 2005; Revised Manuscript Received March 13, 2006

ABSTRACT: Maleated ethylene/propylene copolymers (MAn-*g*-EPM) were thermoreversibly cross-linked via a reaction with primary alkylamines of different length, either with an equimolar amount to obtain the amide−acid or with an excess to obtain the amide−salt, which was confirmed using Fourier transform infrared (FTIR) spectroscopy. Small-angle X-ray scattering (SAXS) experiments showed the presence of microphase-separated aggregates for both the starting MAn-*g*-EPM and all alkylamide−acids and −salts, which act as physical cross-links. The materials could easily be remolded at 80 °C into homogeneous films for several times without changes in the FTIR spectra, indicating that the (physical) cross-links are truly reversible. The tensile properties and elasticity were improved by converting MAn-*g*-EPM to the amide−acids due to hydrogen bonding and even further by converting the amide−acids to the amide−salts due to additional ionic interactions besides hydrogen bonding. Better tensile properties and elasticity were observed for the octadecylamine, which was explained by packing of the long alkyl tails in a crystalline-like order. Apparently, this packing is rather ill-defined, since a scattering peak could only be observed in the SAXS patterns of material modified with a large excess of octadecylamine after processing above 140 °C. Irreversible imide formation occurred for all amide−acids and amide−salts at high temperatures, resulting in disappearance of the aggregates and, hence, a dramatic decrease in mechanical properties. Therefore, these temperatures should be avoided during the (re)processing. Replacement of the excess of alkylamine with a different base, viz. potassium hydroxide, resulted in prevention of imide formation at high temperatures and a further improvement in mechanical properties.

Introduction

Elastomers are used in a wide range of applications, such as tires, tubes, seals, gloves, boots, and toys. Cross-linking of elastomers is necessary to obtain the typical rubber properties, like elasticity, high elongation at break, and good swelling resistance. However, the main technologies for rubber cross-linking, i.e., sulfur vulcanization and peroxide curing, involve irreversible cross-linking, which prevents melt processing and strongly complicates recycling of scrap material and used products.[1]

A solution to overcome this (recycling) problem is to develop elastomers with a thermoplastic behavior, so-called thermoplastic elastomers (TPEs). TPEs are materials which, in the ideal case, combine the service properties of elastomers with the melt processing properties of thermoplastics. The cross-links in these materials are thermoreversible; i.e., they behave as true cross-links at application temperature but weaken or disappear at high temperatures and re-form again upon cooling.[2] The cross-links in TPEs can be of physical nature, based on phase separation, crystallization, ionic interactions and/or hydrogen bonding, or chemical nature, i.e., reversible covalent bonds. Most commercial TPEs are block copolymers consisting of hard and soft blocks, such as polystyrene−polybutadiene−polystyrene triblock copolymers (SBS). Below the glass transition temperature, the polystyrene blocks form rigid domains within the soft polybutadiene matrix, which act as physical cross-links, but become rubbery at elevated temperatures, enabling melt processing.

Ionomers are another class of materials with thermoreversible cross-links. These are ion-containing polymers with a relatively small fraction of ionic groups either pendant to or incorporated in the apolar main chains. The ionic groups tend to form microphase-separated ionic aggregates that act as physical cross-links.[3−7] The existence of ionic aggregates has been shown for many ionomers, mainly using small-angle X-ray scattering (SAXS). The SAXS pattern of an ionomer generally contains an "ionic" peak originating from the ionic aggregates at q values of 0.1−0.4 Å^{-1}, where q is the scattering vector ($q = (4\pi/\lambda) \sin\theta$, where λ is the X-ray wavelength and 2θ is the scattering angle). The reversibility of the ionic cross-linking is based on the increased mobility of the ionic aggregates at elevated temperature.

Hydrogen bonding can also be used for thermoreversible cross-linking, since hydrogen bonds weaken at elevated temperatures. The strength of a single hydrogen bonding donor and acceptor pair is only limited, but it is in principle relatively easy to improve the strength of hydrogen bonds by combining them in arrays of hydrogen-bonding sites.[8] Stadler and co-workers reported on polybutadiene-based thermoplastic elastomers, which were cross-linked using a double-hydrogen-bonding array between grafted phenyl urazole groups, leading to improved properties compared to the unmodified polybutadiene.[9,10] However, the viscoelastic properties were limited due to the weak

† Fudan University.
‡ Eindhoven University of Technology.
§ Dutch Polymer Institute.
⊥ DSM Research.
* Corresponding author: e-mail J.G.P.Goossens@tue.nl; Tel +31 40 2473899; Fax +31 40 2436999.

10.1021/ma052691v CCC: $33.50
Published on Web 04/08/2006

Scheme 1. Reaction Scheme for the Modification of MAn-*g*-EPM with Primary Amines

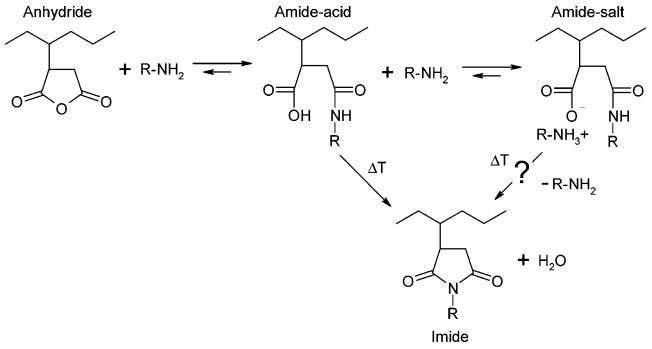

association constant of phenylurazoles (10^2 L/mol in chloroform).[11] Loontjens et al. prepared reversible polymer networks based on imide-functionalized low molecular weight poly(tetramethylene oxides), which were reversibly cross-linked with melamine via the well-known imide−diaminopyridine triple-hydrogen-bonding array.[12] These materials showed a rheological behavior typical of covalent polymer networks. Meijer and co-workers obtained reversible polymer networks using the strongly dimerizing, quadruple-hydrogen-bonding ureido−pyrimidone unit.[13] Their materials possessed viscoelastic properties without the need for additional stabilization by phase separation, and the hydrogen-bonding strength was sufficient to obtain acceptable mechanical properties. Recently, Bouteiller and co-workers studied thermoplastic elastomers based on poly(dimethylsiloxanes) with grafted bisurea groups, which underwent strong, reversible self-association, resulting in impressive viscoelastic and tensile properties.[14] Chino et al. reported on thermoreversibly cross-linked rubbers obtained by modification of the rubber with maleic anhydride (MAn), followed by a reaction with 3-amino-1,2,4-triazole.[15] The authors speculated on a six-point hydrogen-bonding structure, leading to acceptable mechanical properties, while processing could be repeated at least 10 times without affecting the properties.

During previous studies in our group, ionomeric thermoplastic elastomers based on maleated ethylene/propylene copolymers (MAn-*g*-EPM) were studied. These ionomers exhibited good mechanical properties but rather high melt viscosities due to the very strong ionic interactions.[16−18]

This paper presents our continuing work on thermoreversible cross-linking of the same starting material, MAn-*g*-EPM, albeit with a higher molecular weight and a lower degree of grafting, now using either hydrogen bonding or a combination of hydrogen-bonding and ionic interactions. The MAn-*g*-EPM itself is unable to form hydrogen bonds, since the grafted maleic anhydride groups do not possess a hydrogen bond donor. An equimolar amount of a primary alkylamine is used to open the anhydride rings, thereby forming an amide−acid structure[19−21] (Scheme 1), to introduce the possibility of intermolecular hydrogen bonding to cross-link the rubber. Primary aliphatic amines are used because of their fast reaction in solution with anhydride groups at low temperatures, without the need for a catalyst.[19−21] The reaction with amines has been used extensively for maleic anhydride copolymers, mainly for poly(styrene-*co*-maleic anhydride) (SMA),[21−26] but also for copolymers of maleic anhydride with ethylene[25,27] or propylene,[26,28] usually to obtain maleimide copolymers. It is well known that the amide−acid undergoes ring closure to form an imide structure at elevated temperatures (Scheme 1).[19−22] In our case, imide formation leads to a loss of hydrogen-bonding capability, and hence, a deterioration of properties can be expected. This would severely limit the processing temperature window for these materials.

The amide−acid structure has a carboxylic acid functionality that can be neutralized to introduce additional ionic interactions. Primary amines can be used to neutralize carboxylic acid groups,[29,30] so the addition of an excess of primary amine to MAn-*g*-EPM will lead to the formation of an amide−salt structure with an alkylammonium ion as counterion (Scheme 1), which is able to form both hydrogen bonds and ionic interactions. The presence of these (relatively strong) ionic interactions for the amide−salts might prevent the imide formation.

The effect of the type and amount of primary amine on the morphology, studied by SAXS, and the mechanical properties are investigated in order to obtain insight into the cross-linking mechanism(s). Fourier transform infrared (FTIR) spectroscopy is used to study the conversion of MAn-*g*-EPM with amines and to determine the molecular structure of the reaction products. The effect of the processing conditions on the possible imide formation and its effect on the morphology and mechanical properties are studied for both the amide−acids and the amide−salts. Finally, a different base for the conversion of amide−acid to amide−salt, namely potassium hydroxide, is used to explore the effect on the imide formation and the mechanical properties.

Experimental Section

Materials. Maleated ethylene/propylene copolymer (MAn-*g*-EPM, 49 wt % ethylene, 49 wt % propylene, 2.1 wt % maleic anhydride [MAn], $M_n = 40$ kg/mol, $M_w = 90$ kg/mol) was provided by DSM Elastomers and was dried for 1 h at 170 °C under reduced pressure with a low nitrogen flow prior to use to convert all acid groups formed upon hydrolysis back to anhydride. Propylamine (C_3, Aldrich), hexylamine (C_6, Aldrich), decylamine (C_{10}, Aldrich), tetradecylamine (C_{14}, Aldrich), octadecylamine (C_{18}, Aldrich), ammonia (NH_4OH in water, Aldrich), tetrahydrofuran (THF, Biosolve), acetone (Biosolve), and potassium hydroxide (KOH, Merck) were used as received.

Modification. Typically, 10 g of MAn-*g*-EPM was dissolved in 100 g of THF at 60 °C, after which the solution was cooled to room temperature. In parallel, the required amount of alkylamine, calculated from the grafted maleic anhydride content, was dissolved in THF at room temperature. The alkylamine solution was added to the MAn-*g*-EPM solution and mixed for at least 1 h. After the reaction, the products were precipitated in acetone and dried at 40 °C under vacuum. NH_3-saturated MAn-*g*-EPM was prepared by exposing 1 mm thick compression-molded films of MAn-*g*-EPM to a NH_3 atmosphere for several days at room temperature.

For the modification with KOH, typically 5 g of hexylamide−acid, obtained via modification of MAn-*g*-EPM with 1 equiv of hexylamine, was dissolved in 50 g of a toluene/2-propanol mixture (90:10 w/w) at 60 °C, after which the solution was cooled to room temperature. In parallel, the required amount of KOH was dissolved in 2-propanol at room temperature. The KOH solution was added to the hexylamide−acid solution and mixed for at least 1 h. Finally, the solvents were removed by drying at 40 °C under N_2 flow for several days.

Nomenclature. The materials, to which 1 equiv of alkylamine based on the anhydride groups was added, are named alkylamide−acids, for instance propylamide−acid in the case of propylamine. The materials to which two or more equivalents were added are named alkylamide−salts. The products of alkylamide−acids and NH_3-saturated MAn-*g*-EPM after compression molding at 180 °C are referred to as alkylimides and NH_3−imide, respectively.

Compression Molding. The alkylamine-modified materials were compression molded between Teflon sheets at 80 °C to avoid imide formation or at different temperatures to observe the effect of temperature on the imide formation. The KOH-neutralized hexyl-

Table 1. Assignment of the Characteristic Absorption Bands in the FTIR Spectra

wavenumber (cm^{-1})	assignment
1865	anhydride (symmetric) C═O stretch
1785	anhydride (antisymmetric) C═O stretch
1770	imide (symmetric) C═O stretch
1710	acid C═O stretch
1705 (1715)[a]	imide (antisymmetric) C═O stretch
1640 (1665)[a]	amide (I) C═O stretch
1560	carboxylate C═O stretch
1555	amide (II) N−H stretch

[a] Band positions are slightly shifted for the NH_3-saturated materials and are given in parentheses.

amide−acids were compression molded at 180 °C. Heating the samples in a (closed) mold also prevented evaporation of the amines.

Fourier Transform Infrared (FTIR) Spectroscopy. Samples were analyzed on a BioRad Excalibur 3000 spectrometer equipped with a Specac Golden Gate ATR setup over a spectral range of 650−4000 cm^{-1} at a resolution of 4 cm^{-1} coadding 35 scans.

Small-Angle X-ray Scattering (SAXS). SAXS experiments were performed on compression-molded samples on the DUBBLE beamline (BM26) at the European Synchrotron Radiation Facility (ESRF) in Grenoble, France, using a wavelength of 1.2 Å. The data were collected using a 2D multiwire gas-filled detector with pixel array dimensions of 512 × 512. The detector was positioned at 2.5 m from the sample and calibrated using collagen of a rat tail. The exposure time for each sample was 100 s. The experimental data were corrected for background scattering, i.e., subtraction of instrumental errors, and transformed into 1D plots by azimuthal angle integration using the FIT2D program developed by Dr. Hammersley (ESRF).

Dynamic Mechanical Thermal Analysis (DMTA). Rectangular samples with dimensions of 10 × 3 × 1 mm were cut from compression-molded films. A temperature sweep from −100 up to 200 °C at a heating rate of 3 °C/min and a frequency of 1 Hz was performed on a DMA Q800 from TA Instruments with a tension setup.

Tensile Testing. Dumbbell-shaped tensile bars with dimensions of 35 × 2 × 1 mm were punched from compression-molded films. Tensile tests were performed with a constant speed of 0.5 mm/s at room temperature on a Zwick Z010 tensile tester equipped with a force cell of 20 N using TestXpert v7.11 software. All materials were tested in at least 5-fold.

Compression Set (CS). Cylindrical samples with a diameter of 13 mm and a thickness of ∼6 mm were compressed between two parallel plates with a linear deformation of 25% at room temperature for 22 h. The compression set was determined after a relaxation time of 30 min without deformation using eq 1.

$$CS = (t_0 - t_i)/(t_0 - t_n) \times 100\% \quad (1)$$

where t_n is the thickness of the spacer, t_0 is the initial thickness, and t_i the final thickness of the sample.

Results and Discussion

Formation of Amide−Acids and Amide−Salts. Chemistry. The amount of alkylamine added to MAn-*g*-EPM has an important influence on the structure of the functional groups; i.e., it determines whether an amide−acid or an amide−salt structure is formed (Scheme 1). FTIR spectroscopy can be used to study these structures, since the position and the intensity of the carbonyl (C═O) stretching vibration bands of the grafted MAn groups change upon reaction. An overview of the assignment of the characteristic FTIR bands is given in Table 1. The FTIR spectrum of the dried MAn-*g*-EPM in Figure 1 shows two absorption bands characteristic for saturated, cyclic anhydrides at 1785 cm^{-1} (strong) and 1865 cm^{-1} (weak),

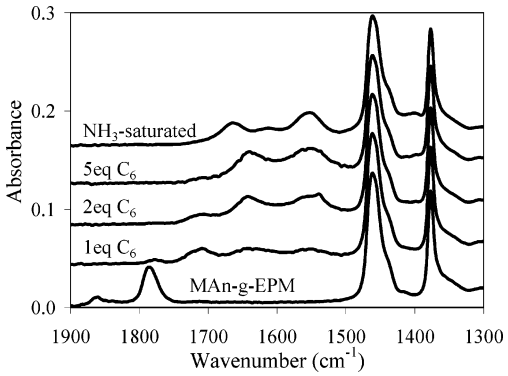

Figure 1. FTIR spectra of MAn-*g*-EPM modified with different amounts of hexylamine (C_6) and an excess of NH_3. The spectra are shifted vertically for clarity.

originating from the antisymmetric and symmetric C═O stretching vibrations, respectively.[20,22,31] No significant formation of intermolecular, acyclic anhydrides takes place, since the characteristic bands around 1820 and 1750 cm^{-1} are not observed.[32−34] Another indication for the absence of intermolecular reactions is the full solubility of MAn-*g*-EPM in THF after drying. The large bands originating from the EPM backbone around 1460 and 1380 cm^{-1}, which can be assigned to the overlapping antisymmetric CH_3 bending and CH_2 scissoring and the symmetric CH_3 bending vibrations of the EPM backbone, respectively,[32] remain unchanged upon reaction and can be used as internal reference.

Figure 1 further shows that three new absorption bands appear upon the addition of 1 equiv of hexylamine to MAn-*g*-EPM, while the intensity of the anhydride bands decreases. The band around 1710 cm^{-1} can be assigned to the C═O stretching vibration of the carboxylic acid and the bands around 1640 and 1555 cm^{-1} to the C═O stretching vibration (amide I) and the NH stretching vibration (amide II) of the amide,[19,21,31] respectively, indicating that the alkylamide−acids are indeed formed. The FTIR spectra of the propyl-, decyl-, tetradecyl-, and octadecylamide−acids are not shown here because the spectra are very similar in this spectral region.

The intensity of the band around 1710 cm^{-1} originating from the carboxylic acid decreases upon addition of 2 equiv of hexylamine, indicating the successful neutralization of the acid groups and the formation of the amide−salt structure. The FTIR spectra do not change significantly upon addition of an excess of hexylamine (5 equiv). The FTIR spectra for the octadecylamide−salts are similar in this spectral region and are not shown here. The spectrum for the NH_3-saturated MAn-*g*-EPM is comparable to that of the hexylamide−salts, except that the amide I band is observed at a higher wavenumber (1715 cm^{-1}) due to the substitution of the alkyl tail by a hydrogen atom and to the presence of additional hydrogen bonding.

Morphology. The morphology will have a significant influence on the final properties of the materials and is studied using small-angle X-ray scattering (SAXS). The SAXS pattern of the dried MAn-*g*-EPM in Figure 2 shows a broad peak around q = 0.06 $Å^{-1}$, which indicates that the MAn-*g*-EPM is already microphase separated. This was also observed during our previous work on MAn-*g*-EPM-based ionomers, which showed a peak at approximately the same position for the ionomer precursor MAn-*g*-EPM.[16−18] The aggregate formation in MAn-*g*-EPM is driven by the large difference in polarity between the polar grafted MAn groups and the apolar EPM chains. It was shown with the help of the Yarusso−Cooper (Y−C) model[35] that the size of the aggregates in MAn-*g*-EPM-based

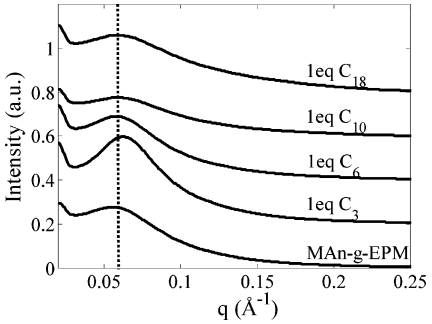

Figure 2. SAXS patterns of MAn-*g*-EPM and different alkylamide-acids, viz. propyl- (C_3), hexyl- (C_6), decyl- (C_{10}), and octadecylamide−acid (C_{18}). The patterns are shifted vertically in steps of 0.2 au for clarity.

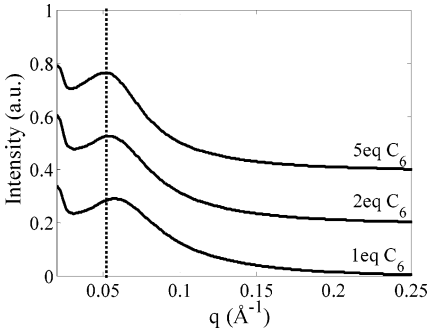

Figure 3. SAXS patterns of MAn-*g*-EPM modified with different amounts of hexylamine (C_6). The patterns are shifted vertically in steps of 0.2 au for clarity.

ionomers is much larger than that for other ionomers. Furthermore, it was concluded that the aggregates contain a substantial amount of EPM chains in addition to the functional groups. The same peak position in the SAXS pattern for the current materials suggests that the aggregates have a comparable, relatively large size and consist of both functional groups and EPM chain parts. In the context of this paper, we do not go into a detailed quantitative analysis of the morphology using the Y−C model but concentrate on relative changes of the scattering curves.

Figure 2 shows that the SAXS patterns of the alkylamide−acids have a broad scattering peak around the same position as MAn-*g*-EPM. The intensity of the scattering peak increases for the propylamide−acid and subsequently decreases for the hexyl-, decyl-, and octadecylamide−acids, while the position of the peak remains more or less the same. This decrease in intensity for the longer alkylamines may be explained by a change in either the composition or the number of the aggregates. The electron density difference between the (initially) polar aggregates and the apolar hydrocarbon matrix is reduced upon incorporation of longer apolar alkyl tails in the aggregates, leading to a decrease in scattered intensity. Alternatively, the polarity difference between the aggregates and the matrix is changed upon the incorporation of longer alkyl tails, which may result in reorganization within the aggregates and/or between the aggregates and the matrix. This reorganization may lead to a lower number of aggregates, most likely of different size, also resulting in a decrease in scattered intensity next to a shift of the scattering peak maximum. Figure 3 shows that the scattered intensity increases when a larger amount of hexylamine is added to MAn-*g*-EPM (2 or 5 equiv), while the peak position remains constant. The same trends occur for the SAXS patterns of the octadecylamide−salts, which are not shown here. The increase in intensity can be related to the larger electron density difference between the functional groups and the matrix because of the introduction of ionic interactions for the amide−salts.

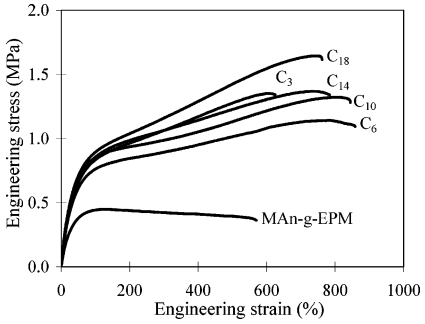

Figure 4. Tensile curves of MAn-*g*-EPM and different alkylamide−acids, viz. propyl- (C_3), hexyl- (C_6), decyl- (C_{10}), tetradecyl- (C_{14}), and octadecylamide−acid (C_{18}).

Table 2. Mechanical Properties of Alkylamine-Modified MAn-*g*-EPM[a]

sample	TS (MPa)	EB (%)	σ_{200} (MPa)	CS (%)
MAn-*g*-EPM (dried)	0.4	560	0.4	88
propylamide−acid	1.3	610	1.0	56
hexylamide−acid	1.1	790	0.8	65
decylamide−acid	1.3	890	0.9	68
tetradecylamide−acid	1.4	800	1.0	67
octadecylamide−acid	1.7	760	1.1	60
hexylamide−salt (2 equiv)	1.4	760	0.9	65
hexylamide−salt (5 equiv)	2.0	870	1.0	64
octadecylamide−salt (2 equiv)	2.9	490	1.8	33
octadecylamide−salt (5 equiv), 80 °C[b]	4.8	620	2.1	25
octadecylamide−salt (5 equiv), 100 °C[b]	3.9	640	1.9	27
octadecylamide−salt (5 equiv), 120 °C[b]	3.5	830	1.6	26
octadecylamide−salt (5 equiv), 140 °C[b]	1.6	490	1.3	36
octadecylamide−salt (5 equiv), 160 °C[b]	0.4	310	0.4	82
octadecylamide−salt (5 equiv), 180 °C[b]	0.2	350	0.2	84
NH_3-saturated MAn-*g*-EPM	4.6	480	2.0	24
NH_3-saturated MAn-*g*-EPM[c]	3.7	520	1.7	
propylimide	0.1	410	0.2	100
octadecylimide	0.1	370	0.2	100
NH_3−imide	0.7	440	0.7	76
hexylamide−acid with 1 equiv of KOH	3.2	690	1.2	24
hexylamide−acid with 2 equiv of KOH	5.2	820	1.4	21

[a] The relative standard deviation is 1−10% for the TS, 3−10% for the EB, and 1−4% for the σ_{200}. [b] Samples were compression molded at different temperatures. [c] Sample was exposed to a normal atmosphere for 5 days.

Mechanical Properties. It was shown in the previous section that the starting MAn-*g*-EPM is already microphase separated into anhydride-rich domains, which act as physical cross-links. The aggregates are also present after modification to amide−acids or amide−salts. Therefore, it is expected that additional hydrogen bonding for the amide−acids and hydrogen-bonding and ionic interactions for the amide−salts will increase the strength of the aggregates, which should improve the mechanical properties, i.e., tensile properties and elasticity, significantly. It should be noted here that all amide−acids and amide−salts can be easily compression molded at 80 °C. The octadecylamide−acid and octadecylamide−salt with 5 equiv are subjected to repeated cycles of cutting the samples in small pieces followed by compression molding at 80 °C. After each cycle, up to four times, fully "healed" films are obtained, for which the FTIR spectra do not change, indicating that the cross-links for these materials, i.e., microphase separation, hydrogen-bonding, or polar and/or ionic interactions, are indeed thermoreversible.

Figure 4 shows representative tensile curves for the alkylamide−acids, while Table 2 shows the average values of the tensile strength (TS), elongation at break (EB), modulus at 200% strain (σ_{200}), and the compression set (CS) for all materials. The

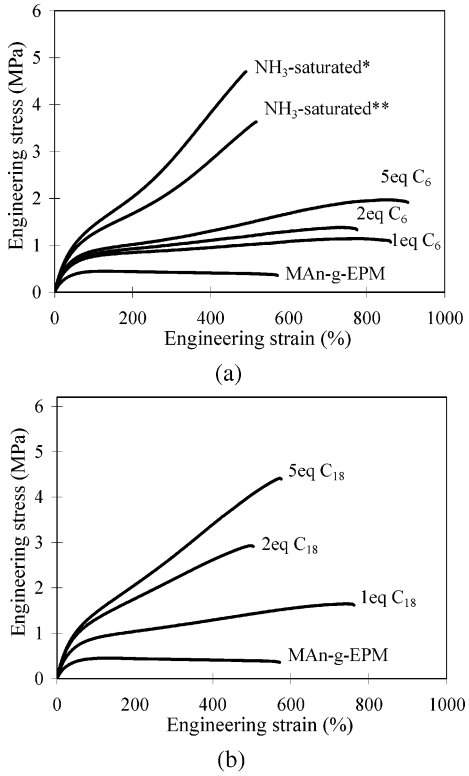

Figure 5. Tensile curves of MAn-*g*-EPM (a) modified with different amounts of hexylamine (C_6) and saturated with NH_3 (*, directly out of NH_3 atmosphere; **, after exposure to normal atmosphere for 5 days) and (b) modified with different amounts of octadecylamine (C_{18}).

compression set is a measure for the elasticity of the material. A compression set of 0% indicates that the material is fully elastic, while a value of 100% indicates a fully inelastic material. All alkylamide−acids have significantly improved tensile properties and a lower compression set, indicating improved elasticity, compared to MAn-*g*-EPM, due to additional hydrogen bonding. The length of the alkyl tail of the primary amine has an important influence on the tensile properties, as shown in Figure 4. However, the trends in tensile properties, i.e., $C_{18} > C_3 \approx C_{14} > C_{10} > C_6$, are not simply following the tail length of the primary amines, which can be explained by the occurrence of two competing effects. The first effect is that longer apolar tails will disturb the aggregate formation, leading to poorer properties, which explains the decrease in properties for the hexylamide−acid compared to the propylamide−acid. Second, the longer tails may organize themselves in a crystalline-like order, which will improve the properties. A better and stronger packing can be expected for the longest alkyl-tails, which may explain the trend $C_{18} > C_{14} > C_{10} > C_6$. It has to be noted that no indication of this "crystallization" could be observed in the SAXS patterns of the decyl- or octadecylamide−acid (Figure 2). Possible reasons could be that the packing of the tails is rather ill-defined or that the amount of amine added is too low to be visible in the SAXS pattern, while the annealing time and temperature are also influencing the organization/crystallization. A comparable trend can be observed for the elasticity as measured by the compression set, i.e., initially poorer elasticity for longer alkylamines, followed by an improvement for the longest amines, which can be explained by the two competing effects described above.

Figure 5 and Table 2 show that the tensile properties for the hexyl- and octadecylamide−salts with 2 and 5 equiv are improved compared to amide−acids, which is related to the introduction of ionic interactions besides hydrogen bonding upon addition of 2 or more equiv of primary amine (Scheme 1), leading to stronger and more stable cross-linking units. A further excess of primary amines can be incorporated in the aggregates as well, where it may strengthen the aggregates via polar interactions, leading to even better properties. A comparison of the hexyl- and octadecylamide−salts in Figure 5 shows that the tensile properties are significantly better for the octadecylamide-salts. The minor improvement in tensile properties and the unaffected elasticity (Table 2) for the hexylamide−salts compared to the hexylamide−acid can be related to the disturbing effect of the apolar hexylamine tails on the aggregate formation, which overrules the positive effect of the additional ionic interactions to a large extent. The larger improvement in tensile properties and elasticity for the octadecylamide−salts may be related to the packing of the long octadecylamine tails in a crystalline-like fashion within the aggregates, which may strengthen the aggregates and improve the properties. This explanation is supported by results obtained from DMTA. Figure 6 shows the storage modulus as a function of temperature for MAn-*g*-EPM, octadecylamide−acid, the octadecylamide−salts, and octadecylimide. The large transition around −50 °C for all materials is the glass transition temperature of the EPM backbone. The transition around 55 °C for the octadecylamide−salts can be attributed to disordering of the packed octadecylamine tails (melting), since this is close to the reported melting temperature of pure octadecylamine (50−54 °C), while no such transition can obviously be observed for the hexylamide−salts, which are not shown here. The transition at 0 °C is caused by melting of traces of absorbed water. The increase in modulus for the octadecylamide−salt with 5 equiv around 120 °C may be related to reorganization within the aggregates. Note that no sign of this organization of the octadecylamine tails is visible in the SAXS patterns for the octadecylamide−salts (Figure 3).

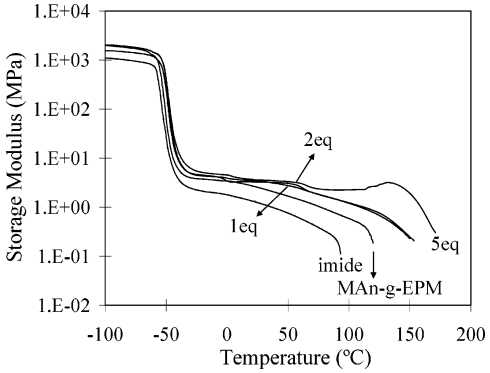

Figure 6. Storage modulus as a function of temperature for MAn-*g*-EPM, MAn-*g*-EPM modified with different amounts of octadecylamine (C_{18}), and octadecylimide.

Figure 6 further shows that the rubbery plateau modulus, which is a direct measure for the network density, is slightly increased for the octadecylamide−acid and −salts compared to MAn-*g*-EPM, indicating a small increase in the network density upon cross-linking. However, the modulus for the octadecylamide−acid and −salts is approximately the same at room temperature, while the tensile properties and the compression set are substantially different. This suggests that the properties of these materials are not determined by the network density, as is the case for conventionally cross-linked rubbers,[1] but by the strength of the aggregates, which is increased due to the presence of hydrogen-bonding and ionic interactions within the aggregates.

The NH_3-saturated MAn-*g*-EPM has better tensile properties and elasticity than the alkylamide−salts, which is related to the

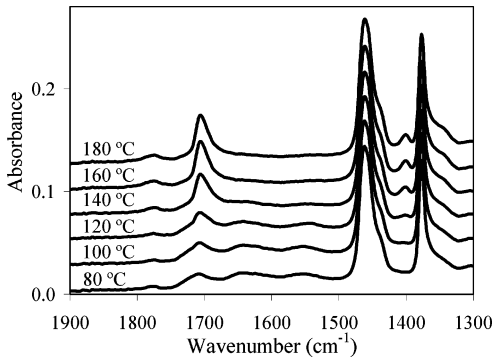

Figure 7. FTIR spectra of hexylamide−acid after compression molding at different temperatures for 20 min. The spectra are shifted vertically for clarity.

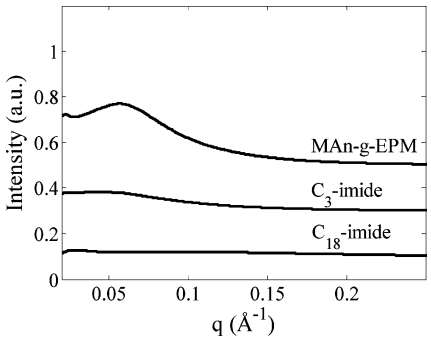

Figure 8. SAXS patterns of MAn-*g*-EPM and propyl- (C_3) and octadecylimide (C_{18}). The patterns are shifted vertically in steps of 0.2 au for clarity.

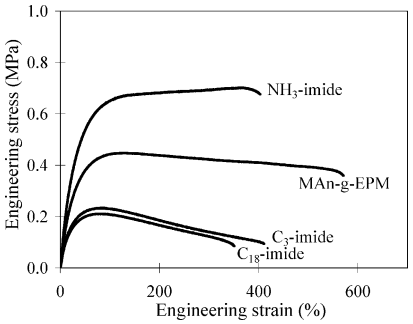

Figure 9. Tensile curves of MAn-*g*-EPM and different imides, viz. NH_3-, propyl- (C_3), and octadecylimide (C_{18}). The materials were compression-molded at 180 °C.

higher polarity of NH_3 compared to the alkylamines, for which the aggregates are disrupted to a certain extent, and the larger extent of hydrogen bonding. However, a main concern is the high volatility of NH_3, which leads to evaporation out of the rubber over time. Figure 5 shows that the tensile properties are already significantly decreased after 5 days when the samples are removed from the NH_3 atmosphere.

At this point, it can be concluded that the tensile properties are significantly improved when MAn-*g*-EPM is modified with primary amines, especially in the case of large amounts of octadecylamine and NH_3. However, imide formation may occur for the amide−acids and possibly the amide−salts at elevated temperatures. The next section deals with the influence of (high temperature) compression molding on the structure and the properties of both the amide−acids and the amide−salts.

Imide Formation. Imide Formation for the Amide−Acids. Figure 7 shows the FTIR spectra for the hexylamide−acid after compression molding at temperatures varying from 80 to 160 °C for 20 min. The spectra do not change significantly up to 120 °C, indicating that the amide−acid prevails. A sharp band around 1705 cm^{-1} appears at 140 °C and higher, which can be assigned to the antisymmetric C═O stretching vibration of the imide,[19,20,22] while the bands around 1640 and 1555 cm^{-1}, assigned to amide I and II, decrease with increasing temperature. This indicates that significant imide formation occurs above 140 °C for the hexylamide−acid. The imide formation is complete at 160 and 180 °C. Note that the (weak) band for the symmetric C═O stretching vibration of the imide, usually present around 1770 cm^{-1}, cannot be observed here due to overlap with the antisymmetric C═O stretching vibration of the residual anhydride groups at 1785 cm^{-1}. Formation of intermolecular, acyclic imides does not occur significantly, since no additional band at lower wavenumbers, i.e., around 1670−1690 cm^{-1}, can be observed.[36] In addition, the materials are still fully soluble in THF after imide formation, indicating the absence of intermolecular linkages. A new band appears around 1400 cm^{-1} for the alkylimides, which can be assigned to the C−N−C bending of the imide ring.[32] Full imide formation occurs also for the propyl- and octadecylamide−acids after compression molding at 180 °C (not shown here).

Additional experiments show that the FTIR spectra remain unchanged for the hexylamide−acid after compression molding at 80 and 100 °C, even after 4 h, indicating that no imide formation takes place at these temperatures. However, some imide formation occurs after compression molding at 120 °C for 1 h, which becomes more extensive after longer times. Unfortunately, a quantitative analysis of the imide formation is difficult due to the significant overlap of the bands for the acid at 1710 cm^{-1} and the imide at 1705 cm^{-1}. In conclusion, high temperatures should be avoided during the (re)processing of these materials, since this would lead to irreversible imide formation.

The SAXS patterns of the imides in Figure 8 show that no aggregates exist in the propyl- and octadecylimide materials. The formation of the alkyl N-substituted imide drastically decreases the polarity of the functional groups compared to the amide−acid, leading to the disappearance of the aggregates for the alkylimides, as the tendency for microphase separation is strongly reduced. As a consequence, the network density is significantly decreased, resulting in a significant drop in rubbery plateau modulus for the octadecylimide, as shown in Figure 6. The tensile properties of the imides (Figure 9 and Table 2) decrease to a level even below the starting MAn-*g*-EPM material due to the disappearance of the aggregates, since no cross-linking mechanism seems to be present anymore. Similarly, the compression set for the alkylimides is 100%, indicating that the materials do not behave elastically anymore.

Imide Formation for the Amide−Salts. Figure 10 shows the FTIR spectra of the hexyl- and octadecylamide−salts with 2 and 5 equiv and the NH_3-saturated MAn-*g*-EPM after compression molding at 180 °C. The disappearance of the amide I and II bands at 1645 and 1555 cm^{-1}, respectively, and the appearance of a new sharp peak at 1705 cm^{-1} indicate that full imide formation took place for the hexylamide−salts and the NH_3-saturated MAn-*g*-EPM, which is further referred to as NH_3−imide. The (imide) band for the NH_3−imide is observed at a higher wavenumber (1715 cm^{-1}) compared to the alkylimides due to the ability to form hydrogen bonds.

Three new bands at 1645, 1590, and 1565 cm^{-1} appear in the FTIR spectra for the octadecylamide−salts, while the band at 1460 cm^{-1} originating from the CH_3-bending and CH_2-scissoring vibrations of the aliphatic part splits up into multiple bands. The intensity of the imide band is significantly lower for the octadecylamide−salt with 5 equiv than for the other

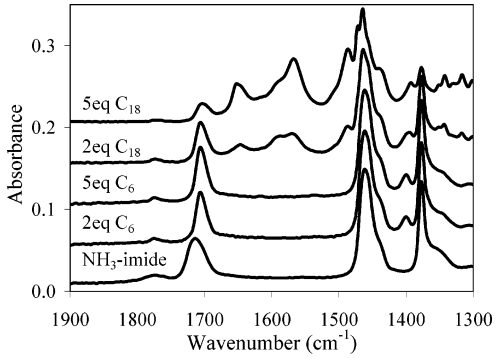

Figure 10. FTIR spectra of hexyl- (C_6) and octadecylamide−salts (C_{18}) with 2 and 5 equiv and NH_3-saturated MAn-*g*-EPM after compression molding at 180 °C. The spectra are shifted vertically for clarity.

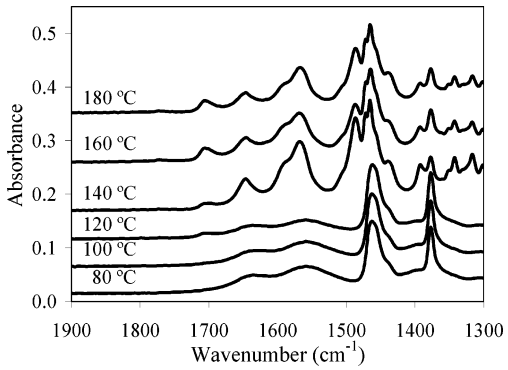

Figure 11. FTIR spectra of the octadecylamide−salt with 5 equiv after compression molding at different temperatures. The spectra are shifted vertically for clarity.

materials. Figure 11 shows the FTIR spectra for samples of the octadecylamide−salt with 5 equiv after compression molding at various temperatures. The spectra do not change significantly after compression molding at temperatures up to 120 °C, indicating that the amide−salt prevails. The appearance of the new bands, the splitting of the band at 1460 cm^{-1}, and the imide formation start to occur after compression molding at temperatures of 140 °C and higher.

The splitting of the band at 1460 cm^{-1} can be attributed to the packing of the octadecylamine tails in a crystalline-like order having an all-trans conformation, such as observed for e.g. polyethylene.[37−39] The bands at 1645, 1590, and 1565 cm^{-1} also appear for the pure octadecylamine after heating to 60 °C (solid−solid transition), while they disappear again upon melting after heating to 80 °C. Heating the octadecylamide−salt with 5 equiv, which was compression molded at 160 °C, to 80 °C leads to the disappearance of these bands as well. These results suggest that the bands are originating from the excess of octadecylamine with an ordered, crystalline-like structure. Additionally, the band at 1460 cm^{-1} regains its original shape after heating at 80 °C, which can be related to the disappearance of the ordered structure. The intensity of the imide band at 1705 cm^{-1} increases to the same level as for the hexylamide−salts compression molded at 180 °C after heating, indicating that full imide formation has occurred for the octadecylamide−salts as well. Note that the FTIR spectra are scaled using the band at 1460 cm^{-1}, which increases in intensity due to the octadecylamine packing, resulting in an apparent decrease in intensity of the imide band.

The SAXS patterns of the amide−salts after compression molding at 180 °C in Figure 12 show that the aggregates have disappeared for all alkylamide−salts due to the imide formation but that aggregates are still present for the NH_3−imide. The

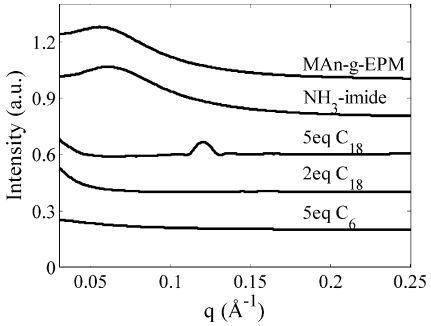

Figure 12. SAXS patterns of the hexylamide−salt (C_6) with 5 equiv and the octadecylamide−salts (C_{18}) with 2 and 5 equiv and the NH_3-saturated MAn-*g*-EPM (NH_3-imide) after compression molding at 180 °C. The patterns are shifted vertically in steps of 0.2 au for clarity.

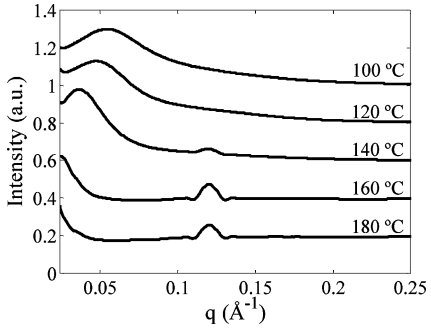

Figure 13. SAXS patterns of the octadecylamide−salt with 5 equiv after compression molding at different temperatures. The patterns are shifted vertically in steps of 0.2 au for clarity.

higher polarity of the NH_3−imide groups compared to the alkylimides and the ability to form hydrogen bonds enable aggregate formation similarly to MAn-*g*-EPM. Therefore, the NH_3−imide has slightly better mechanical properties than MAn-*g*-EPM due to the existence of hydrogen bonding within the still present aggregates, as shown in Figure 9 and Table 2. However, the properties of the NH_3−imide are significantly decreased compared to the NH_3-saturated MAn-*g*-EPM.

Figure 12 further shows that a new sharp peak appears for the octadecylamide−salt with 5 equiv at $q = 0.12$ Å^{-1}, corresponding to a *d*-spacing of 54 Å, which indicates that the octadecylamine molecules pack together in a bilayered structure. This peak cannot be observed for the hexylamide−salts, for which no packing of the chains is expected, and the octadecylamide−salt with 2 equiv, for which the amount of octadecylamine is probably too low to be visible. The SAXS patterns of samples of the octadecylamide−salt with 5 equiv after compression molding at various temperatures in Figure 13 show that the broad peak centered around at $q = 0.06$ Å^{-1} shifts to lower q values for increasing temperatures, indicating changes in the aggregate structure. The aggregates have disappeared for the samples compression molded at 160 and 180 °C due to imide formation. The sharp peak at $q = 0.12$ Å^{-1} appears after compression molding at 140 °C or higher. The fact that this peak only appears in the case of a large excess of octadecylamine after compression molding at temperatures above 140 °C suggests that both a certain amount of octadecylamine and high temperatures are required for a well-ordered packing of the long alkyl tails. The bilayered packing of the octadecylamine molecules implies that the NH_2 end groups are pointing toward each other. The bands at 1645, 1590, and 1560 cm^{-1} are believed to originate from interactions or even (reversible) reactions between the NH_2 groups within the ordered structure, such as carbamic acid formation with CO_2.

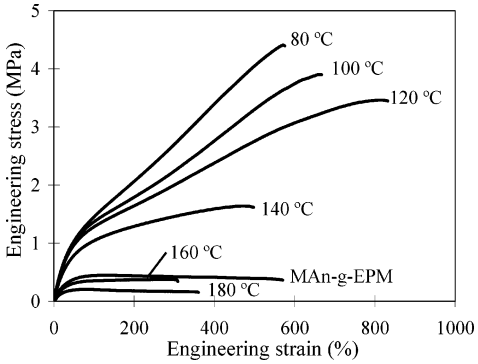

Figure 14. Tensile curves of the octadecylamide−salt with 5 equiv after compression molding at different temperatures.

Figure 14 and Table 2 show the tensile properties of samples of the octadecylamide−salt with 5 equiv after compression molding at various temperatures. The properties deteriorate slightly for the samples compression molded at 100 and 120 °C, in which the amide−salt is still present. This decrease is most probably related to changes in the aggregate structure. A significant decrease in properties occurs for the sample compression molded at 140 °C, for which some imide formation has occurred. The properties of the samples compression molded at 160 and 180 °C become even poorer than for the starting MAn-*g*-EPM because the aggregates have disappeared completely, similarly to the octadecylimide (Figure 9). The compression set measurements in Table 2 show a comparable trend; i.e., the elasticity is hardly affected for the samples compression molded at 80, 100, and 120 °C but becomes significantly poorer at 140 °C and goes to a level only slightly better than that of MAn-*g*-EPM at 160 and 180 °C. Apparently, the packing of the octadecylamine molecules is still taking place, but within a separate phase and consequently does not have an influence on the tensile properties.

Prevention of Imide Formation. It was shown earlier that imide formation at elevated temperatures leads to a dramatic decrease in properties (Figure 9). The introduction of additional ionic interactions for the alkylamide−salts could not prevent the imide formation. The reason for this might be that the ionic interactions in the amide−salts are not strong enough. Weiss et al.[29] showed for sulfonated polystyrene ionomers that ionic interactions are significantly stronger for metal counterions than for primary alkylammonium ions, while Xie et al.[30] showed the same for sulfonated butyl rubbers. Therefore, potassium hydroxide (KOH) is used for the neutralization of the carboxylic acid group of the hexylamide−acid, instead of a second (or higher) equivalent of hexylamine, to study whether neutralization with a stronger base and (stronger) ionic interactions with the potassium ions can prevent imide formation. Two different amounts of KOH have been added: 1 equiv, i.e., the stoichiometric amount to neutralize all carboxylic acid groups of the alkylamide−acid, and 2 equiv.

Figure 15 shows that the absorption band at 1710 cm^{-1} originating from the carboxylic acid does not completely disappear for the material with 1 equiv of KOH after drying, indicating that some residual hexylamide−acid groups are present. A new band appears around 1560 cm^{-1}, which is assigned to the carboxylate.[18] A small band around 1705 cm^{-1} is visible after compression molding at 180 °C, indicating that only a limited amount of imide formation took place. The dried material contains some residual hexylamide−acid, which is easily converted into imide upon heating (Figure 7). The carboxylic acid band is even smaller for the material modified

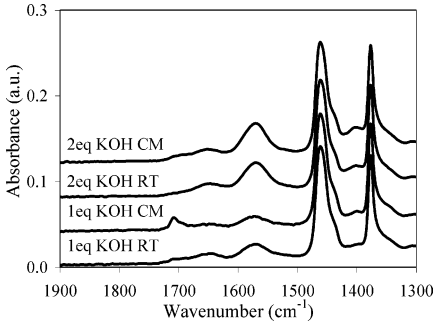

Figure 15. FTIR spectra of hexylamide−acid neutralized with 1 and 2 equiv of KOH measured after drying (RT) and after compression molding at 180 °C (CM). The spectra are shifted vertically for clarity.

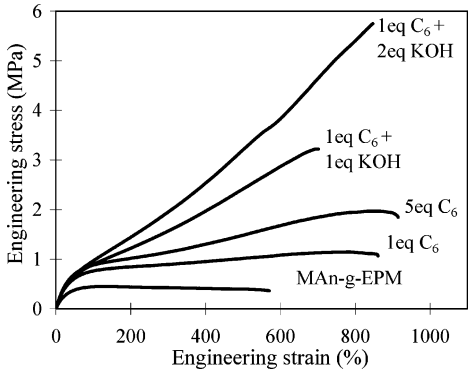

Figure 16. Tensile curves of hexylamide−acid neutralized with 1 and 2 equiv of KOH and the hexylamide−salt with 5 equiv.

with 2 equiv of KOH after drying, which shows that almost all amide−acid groups are converted to amide−salt. The FTIR spectrum remains unaffected after compression molding, indicating that imide formation is fully suppressed.

The tensile properties and the elasticity as measured by the compression set of the KOH-neutralized hexylamide−acids in Figure 16 and Table 2 are significantly better than for the hexylamide−salt with 5 equiv. The material with 2 equiv of KOH gives better properties than with 1 equiv of KOH, which indicates that the excess of KOH further strengthens the aggregates. The ionic interactions with potassium as counterion are indeed much stronger than in the case of primary alkylammonium ions, which is in agreement with observations in the literature,[29,30] leading to both prevention of imide formation and better mechanical properties.

Conclusions

In this work, MAn-*g*-EPM is thermoreversibly cross-linked using various amounts of different alkylamines. The addition of 1 equiv of alkylamine results in the formation of an amide−acid structure, which is able to form hydrogen bonds, while the addition of an excess (2 equiv or more) leads to the neutralization of the carboxylic acid group of the amide−acid and the formation of an amide−salt structure, for which hydrogen bonding is combined with ionic interactions. Microphase-separated aggregates are present for the MAn-*g*-EPM, the amide−acids, and the amide−salts, which act as physical cross-links. The materials could easily be remolded at 80 °C into homogeneous films for several times, without changes in the FTIR spectra, indicating that the (physical) cross-links, i.e., aggregation, hydrogen-bonding, and polar or ionic interactions, are indeed reversible.

The tensile properties and the elasticity of the amide−acids are significantly improved compared to MAn-*g*-EPM due to the

presence of hydrogen bonding within the aggregates. The trend of an initial decrease for longer alkylamines followed by an improvement for the longest amines is explained by two competing effects, namely disruption of the aggregates by longer apolar alkyl tails and packing of long tails in a crystalline-like order. This packing is apparently rather ill-defined, which explains why no sign of this packing is visible in the SAXS patterns. The properties improve further for the amide−salts due to the presence of additional ionic interactions, with better properties for the octadecylamide−salts compared to the hexylamide−salts. The best properties are obtained for the NH_3-saturated MAn-*g*-EPM, but a major problem is the high volatility of NH_3, which leads to a significant drop in tensile properties already after 5 days in a normal atmosphere.

An important concern is the occurrence of imide formation for all amide−acids and amide−salts after compression molding at temperatures of 120 °C and higher, resulting in disappearance of the aggregates and poor mechanical properties. Therefore, these temperatures should be avoided during the (re)processing of these materials. A new sharp peak can be observed in the SAXS pattern for the octadecylamide−salt with 5 equiv after compression molding at temperatures of 140 °C and higher, which indicates packing of octadecylamine molecules in a bilayered structure. Finally, the imide formation can be prevented by using a different base, i.e., KOH, for the neutralization of the carboxylic acid group of the hexylamide−acid. The mechanical properties are significantly improved for the KOH-neutralized materials compared to the hexylamide−salts. This is related to the stronger ionic interactions with metal cations than with primary alkylammonium ions.

Acknowledgment. We thank the staff of the DUBBLE beamline (BM26) at the European Synchrotron Radiation Facility (ESRF) in Grenoble, France, for the possibility to perform the SAXS experiments. Furthermore, we thank the Dutch Polymer Institute (DPI) for financial support under Project 346 and the Netherlands Organization for Scientific Research (NWO) for travel and research funding.

References and Notes

(1) *Rubber Technology Handbook*; Hofmann, W., Ed.; Hanser Publishers: Munich, 1989.
(2) *Thermoplastic Elastomers: A Comprehensive Review*; Holden, G., Legge, N. R., Quirk, R. P., Eds.; Hanser: Munich, 1996.
(3) *Introduction to Ionomers*; Eisenberg, A., Kim, J. S., Eds.; John Wiley & Sons: New York, 1998.
(4) *Ionic Polymers*; Holliday, L., Ed.; Applied Science Publishers: London, 1975.
(5) *Ions in Polymers*; Eisenberg, A., Ed.; American Chemical Society: Washington, DC, 1980.
(6) *Ionomers: Characterizations, Theory and Applications*; Schlick, S., Ed.; CRC Press: Boca Raton, FL, 1996.
(7) *Ionomers: Synthesis, Structure, Properties and Applications*; Tant, M. R., Mauritz, K. A., Wilkes, G. L., Eds.; Chapman & Hall: London, 1997.
(8) Sijbesma, R. P.; Meijer, E. W. *Chem. Commun.* **2003**, 5−16.
(9) Stadler, R.; de Lucca Freitas, L. L. *Colloid Polym. Sci.* **1986**, *264*, 773−778.
(10) Müller, M.; Stadler, R.; Kremer, F.; Williams, G. *Macromolecules* **1995**, *28*, 6942−6949.
(11) de Lucca Freitas, L. L.; Auschra, C.; Abetz, V.; Stadler, R. *Colloid Polym. Sci.* **1991**, *269*, 566−575.
(12) Loontjens, T.; Put, J.; Coussens, B.; Lange, R.; Palmen, J.; Sleijpen, T.; Plum, B. *Macromol. Symp.* **2001**, *174*, 357−371.
(13) Lange, R. F. M.; van Gurp, M.; Meijer, E. W. *J. Polym. Sci., Part A: Polym. Chem.* **1999**, *37*, 3657−3670.
(14) Colombani, O.; Barioz, C.; Bouteiller, L.; Chaneac, C.; Fomperie, L.; Lortie, F.; Montes, H. *Macromolecules* **2005**, *38*, 1752−1759.
(15) Chino, K.; Ashiura, M. *Macromolecules* **2001**, *34*, 9201−9204.
(16) Wouters, M. E. L.; Goossens, J. G. P.; Binsbergen, F. L. *Macromolecules* **2002**, *35*, 208−216.
(17) Wouters, M. E. L.; Litvinov, V. M.; Binsbergen, F. L.; Goossens, J. G. P.; van Duin, M.; Dikland, H. G. *Macromolecules* **2003**, *36*, 1147−1156.
(18) Wouters, M. E. L. Ph.D. Thesis, Eindhoven University of Technology, Eindhoven, The Netherlands, 2000.
(19) Schmidt, U.; Zschoche, S.; Werner, C. *J. Appl. Polym. Sci.* **2003**, *87*, 1255−1266.
(20) Padwa, A. R.; Macosko, C. W.; Wolske, K. A.; Sasaki, Y. *Polym. Prepr. (Am. Chem. Soc., Div. Polym. Chem.)* **1993**, *34*, 842−843.
(21) Hu, G. H.; Lindt, J. T. *Polym. Bull. (Berlin)* **1992**, *29*, 357−363.
(22) Vermeesch, I.; Groeninckx, G. *J. Appl. Polym. Sci.* **1994**, *53*, 1365−1373.
(23) Lee, S.-S.; Ahn, T. O. *J. Appl. Polym. Sci.* **1999**, *71*, 1187−1196.
(24) Schmidt-Naake, G.; Becker, H. G.; Klak, M. *Macromol. Symp.* **2001**, *163*, 213−234.
(25) Raetzsch, M.; Phien, V. *Faserforsch. Textiltech., Z. Polymerforsch.* **1976**, *27*, 353−356.
(26) Raetzsch, M.; Krahl, K. *Acta Polym.* **1985**, *36*, 91−95.
(27) Tsuwi, J.; Appelhans, D.; Zschoche, S.; Friedel, P.; Kremer, F. *Macromolecules* **2004**, *37*, 6050−6054.
(28) Raetzsch, M.; Hue, N. T. *Acta Polym.* **1979**, *30*, 93−97.
(29) Weiss, R. A.; Agarwal, P. K.; Lundberg, R. D. *J. Appl. Polym. Sci.* **1984**, *29*, 2719−2734.
(30) Xie, H.; Xu, J. *Angew. Makromol. Chem.* **1990**, *174*, 177−187.
(31) Bayer, T.; Eichhorn, K. J.; Grundke, K.; Jacobasch, H. J. *Macromol. Chem. Phys.* **1999**, *200*, 852−857.
(32) *The Handbook of Infrared and Raman Characteristic Frequencies of Organic Molecules*; Lin-Vien, D., Ed.; Academic Press: Boston, 1991.
(33) Dauben, W. G.; Epstein, W. W. *J. Org. Chem.* **1959**, *24*, 1595−1596.
(34) Bellamy, L. J.; Connelly, B. R.; Philpotts, A. R.; Williams, R. L. *Z. Elektrochem.* **1960**, *64*, 563−566.
(35) Yarusso, D. J.; Cooper, S. L. *Macromolecules* **1983**, *16*, 1871−1880.
(36) Shalaby, S. W.; McCaffery, E. L. *Anal. Chem.* **1968**, *40*, 823−825.
(37) Tasumi, M.; Krimm. S. *J. Polym. Sci., Polym. Phys. Ed.* **1968**, *6*, 995−1010.
(38) Bank, M. I.; Krimm. S. *J. Polym. Sci., Polym. Phys. Ed.* **1969**, *7*, 1785−1809.
(39) Cheam, T.; Krimm. S. *J. Polym. Sci., Polym. Phys. Ed.* **1981**, *19*, 423−447.

MA052691V